Reactivity of Hydroxyl Radicals on Hydroxylated Quartz Surface. 1. Cluster Model Calculations

Robert Konecny*

National Institute for Occupational Safety and Health, 1095 Willowdale Road, Morgantown, West Virginia 26505-2888

Received: February 27, 2001; In Final Form: April 19, 2001

The interaction of a hydroxyl radical with cluster models of a hydroxylated α-quartz surface was studied by means of density functional calculations. Two molecular models representing isolated (≡Si—OH) and geminal (═Si(OH)$_2$) silanol-terminated quartz surfaces were used. Two reactive sites of the silanol models were investigated: the hydrogen of the silanol group and the surface-approximating silicon atom. The •OH binds weakly to the silanol hydrogen atoms in both models, with a reaction energy of about −7 kcal/mol. The silicon atom in the isolated silanol cluster is not reactive toward the •OH. In contrast, the •OH adsorbs on the Si in the geminal silanol cluster with a reaction energy of −4 kcal/mol. The Si—OSi bond in the resulting pentacoordinated silicon complex is weakened upon the •OH adsorption and can be dissociated. The energy barrier to the dissociation is 4 kcal/mol, and the overall reaction energy is −4 kcal/mol. The dissociation of the Si—OSiH$_3$ bond which mimics the Si—O subsurface bonding in the real quartz surface suggests a possibility of •OH activated quartz surface layer disintegration. The calculated energy barrier in this •OH radical activated process is significantly lower than the predicted energy barrier in the rate determining step in the OH$^-$ catalyzed quartz surface dissolution (19 kcal/mol). The Si—OSi bond rupture followed by formation of a Si—O• radical on the surface may provide a plausible mechanism for reactivation of chemically inert, silanol terminated, aged quartz surfaces.

Introduction

Pathogenicity of silica has been one of the longest and most extensively studied issues in occupational and environmental toxicology. Prolonged inhalation of crystalline silica particles can cause lung inflammation and development of fibrogenic lung disease, and silica has been recently also associated with the development of bronchogenic carcinoma, lung cancer.[1] Although the overall silica toxicity mechanism involves a complex interaction between the crystalline surface, lung lining fluid, biological molecules, and cells, there is a significant amount of experimental evidence suggesting that free radical species and particularly hydroxyl radicals play a major role.[2−16] Because of the complexity of this multistep mechanism and the factors involved, the detailed molecular mechanism of silica cytotoxicity is still not very well understood.

Crystalline silica (SiO_2) exists in many different polymorphic forms with α-quartz being the most common and also one of the most toxic polymorphs.[17] All polymorphs, except stishovite, consist of corner sharing SiO_4 tetrahedra forming a three-dimensional network of Si−O−Si bonds with essentially covalent character. When the silica surface is created, the Si−O bonds are broken, leading in this case to a homolytic cleavage with the generation of free radical Si• and Si−O• species. These silicon surface based free radicals can facilitate hydroxyl radical generation in an aqueous environment via the Fenton-chemistry mechanism[3,12−14] (Scheme 1). Transition metal ions (e.g., iron) which are present on the silica surface in trace amounts as impurities also participate in this mechanism.

SCHEME 1

$$\text{Si–O}\cdot + H_2O \rightarrow \text{SiOH} + \cdot\text{OH}$$

$$\text{Si–O}\cdot + \cdot\text{OH} \rightarrow \text{SiOOH}$$

$$\text{SiOOH} + H_2O \rightarrow \text{SiOH} + H_2O_2$$

$$Fe^{II} + H_2O_2 \rightarrow Fe^{III} + \cdot\text{OH} + OH^-$$

The generated hydroxyl radicals are highly reactive species capable of causing oxidative damage to cellular material adsorbed on or in the near vicinity of the silica surface. This radical mechanism elegantly explains the high toxicity of freshly cleaved silica where there is an abundant amount of Si• and Si−O• surface species. Because of their high reactivity, these silicon-based radicals can react quickly in an aqueous environment or in the presence of water vapor to yield fairly unreactive surface silicon bonded hydroxyl groups, silanols. However, experimental evidence suggests[8,12,13,18] that hydroxyl radicals are generated, although to a lesser degree, even on these aged, silanol terminated silica surfaces where the Si• and Si−O• concentration should be negligible. Castranova et al. performed several in vivo and in vitro experiments[8,12,13,18] where they monitored the decrease of the reactivity and cytotoxicity of freshly ground silica with time. Their results show that the concentration of the silicon-based surface radicals initially decays over time but eventually reaches a constant value. Thus, more detailed information about the interaction of the aged quartz surface with radical species, particularly hydroxyl radicals, could provide significant insight into the overall silica toxicity mechanism.

To gain a better understanding of the hydroxyl radical's reactivity on the silanol-terminated silica surfaces, we performed

* Current address: Keck Center, University of California San Diego, La Jolla, CA 92092-0365.

10.1021/jp010752v
Published on Web 06/08/2001

a series of density functional calculations on cluster models of the hydroxylated α-quartz surface. Relative stabilities of the reactants and products and the corresponding energy barriers and transition states have been determined. Results of these calculations and their relevance to silica toxicity are discussed.

Computational Method

Modeling of extended crystalline systems and surfaces in particular is inherently a computationally demanding effort. One approach to simplify this task is to consider a limited number of atoms around the active surface site and apply theoretical methods to the resulting molecular cluster. Although this cluster approach neglects long-range effects on the electronic properties of the active site, it allows for very accurate prediction of local properties.[19−21]

There are two experimentally observed local configurations of surface silanols: an isolated, single silanol (**1a**), where there is only one hydroxyl group bonded to the surface silicon atom, and geminal silanols (**1b**), with two hydroxyl groups attached to the same surface Si (Si_b and O_b represent bulk Si and O atoms, respectively).[22−24]

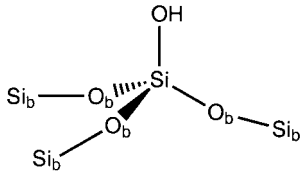

1a

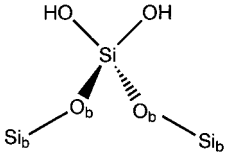

1b

To accurately model these different hydroxylated quartz surface sites, two molecular models were used: isolated (**2a**) and geminal (**2b**) silanol molecular clusters. Both models consist of a central silicon atom approximating the surface silicon, three or two $-O-SiH_3$ groups mimicking the subsurface $-O-Si$ bonding, with silicon unfilled valences saturated by hydrogen atoms, and one or two hydroxyl groups modeling the surface silanols in the isolated and geminal silanol cluster, respectively. These cluster models have been shown to provide a good approximation to the surface.[19−21,25]

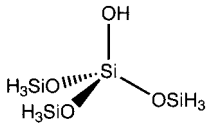

2a

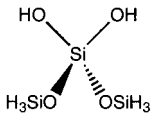

2b

The calculations have been performed using the hybrid B3LYP exchange-correlation functional which includes both local and nonlocal terms.[26,27] The 6-31G** Gaussian basis set was employed with polarization on heavy elements and hydrogen atoms. All degrees of freedom of the studied systems were optimized. Several one-dimensional potential energy surface scans were performed using a single geometrical constraint, bond distance. Transition state searches were carried out using the Berny algorithm.[28] All stable points on the potential energy surface have been verified by full frequency analysis. The calculations were carried out using the Gaussian98 package.[29]

It is important to note that by allowing full optimization of the cluster models we did not take into account any structural constraints imposed on the surface sites by the surrounding crystal lattice in solid quartz. Because of this limitation the predicted energy differences and barriers have to be considered with some care. However, the extent of the molecular models used in our calculations ensures accurate prediction of localized surface events.

Although the calculations were carried out in a vacuum, the presence of a polar solvent in the real environment is not expected to significantly alter predicted reaction energetics for these neutral radical reactions.[30]

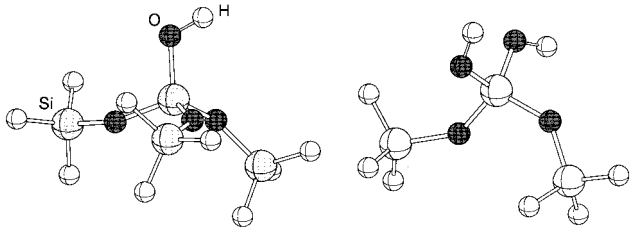

3 **4**

Figure 1. Optimized geometry of isolated (**3**) and geminal (**4**) surface silanol cluster models.

TABLE 1: Optimized Geometrical Parameters of the Isolated (3) and Geminal (4) Silanol Clusters (Bond Lengths in Å and Bond Angles in deg)

	3	**4**
Si−OH	1.644	1.647, 1.643
$Si-OSiH_3$	1.639, 1.638, 1.631	1.641, 1.636
HO−Si−OH		107.4
$HO-Si-OSiH_3$	109.3, 112.5, 107.0	107.7, 113.8 and 106.6, 113.8
$H_3SiO-Si-OSiH_3$	107.8, 108.4, 112.0	107.5
$Si-O-SiH_3$	140.9, 140.2, 143.7	139.7, 139.3

Results and Discussion

The optimized geometries of the two molecular models, isolated (**3**) and geminal (**4**) silanol clusters, are shown in Figure 1, and the key geometrical parameters are presented in Table 1. Both clusters have nearly ideal tetrahedral geometry suggesting that there is no or negligible steric interaction between the ligands. The average values of the $Si-O-SiH_3$ bond angles are 141.6 and 139.5° for the isolated and geminal silanol clusters, respectively. These values are close to the Si−O−Si bond angles in bulk α-quartz (143.7°).[31] The average $Si-OSiH_3$ bond length is 1.64 Å in both molecular models which is only slightly longer than the Si−O bond distance in α-quartz (1.61 Å).[31]

To explore hydroxylated quartz surface reactivity, we theoretically studied several possible mechanisms of hydroxyl radical attack on the surface. Both surface site models, isolated and geminal silanol clusters, have two reactive centers susceptible to attack by the oxygen atom of the hydroxyl radical: the hydrogen atom of the silanol group and the silicon atom attached to the silanols. We have considered reactions on both reactive centers in our modeling.

A. Interaction of a Hydroxyl Radical with Silanol Groups. The hydroxyl radical weakly binds to the hydrogen of the silanol group in both cluster models with similar reaction energies (−6.7 and −6.5 kcal/mol for isolated and geminal silanol clusters, respectively). The distance between the oxygen of the hydroxyl radical and the oxygen of the silanol in the optimized geometry is 2.83 Å, which is a typical value observed in hydrogen bonded systems. The only significant structural change in the cluster geometry upon •OH addition is a slight bond elongation (by 0.01 Å) between the silicon atom and the silanol (Si−OH) group which is involved in the interaction with the hydroxyl radical.

To assess the ability of •OH to abstract hydrogen from a silanol group (Scheme 2), we explored the one-dimensional

SCHEME 2

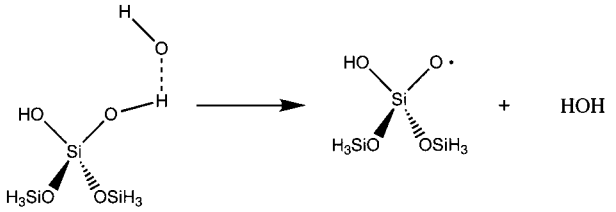

potential energy surface associated with this process. This potential energy profile was calculated by constraining the O−H bond between the approaching hydroxyl radical oxygen atom and silanol hydrogen in the geminal cluster model to several discrete values and performing full optimization of the rest of the cluster at each step. The transition state geometry has also been found and verified by full frequency analysis. The overall hydrogen abstraction reaction is endothermic with a reaction energy of +8.4 kcal/mol. There is also an energy barrier of 10.2 kcal/mol to this process. The leaving hydrogen atom is positioned approximately symmetrically between both oxygen atoms in the transition state geometry with the SiO−HOH and SiOH−OH bond distances 1.18 and 1.15 Å, respectively. The frequency calculation indicates that there is only one imaginary frequency (*i*1409 cm^{-1}) for the transition state structure with the dominant mode being the rupture of the SiO−HOH bond.

These results imply that the silanol hydrogen abstraction by hydroxyl radical and subsequent formation of the siloxyl radical is not an energetically favorable process in our calculation. However, because surface silanols are experimentally known[22−24] to participate in hydrogen bonding to different degrees on different silica surfaces, the interaction between neighboring silanols, which is not accounted for in our cluster models, can have an impact on the total energetics of the silanol hydrogen abstraction. Similar results are expected for abstraction of a hydrogen atom in the isolated silanol group by a hydroxyl radical.

B. Interaction of a Hydroxyl Radical with the Surface Site-Approximating Cluster Silicon Atom. While the hydroxyl radical reacts in similar fashion with silanol hydrogens in both the isolated and geminal silanol sites, there is a significant difference in reactivity between these sites when the hydroxyl radical attacks the silicon atom attached to the silanol group. When the •OH approaches the silicon atom in the isolated silanol cluster, it encounters a repulsive energy barrier (Figure 2); the reaction is endothermic. The most likely origin of the repulsive

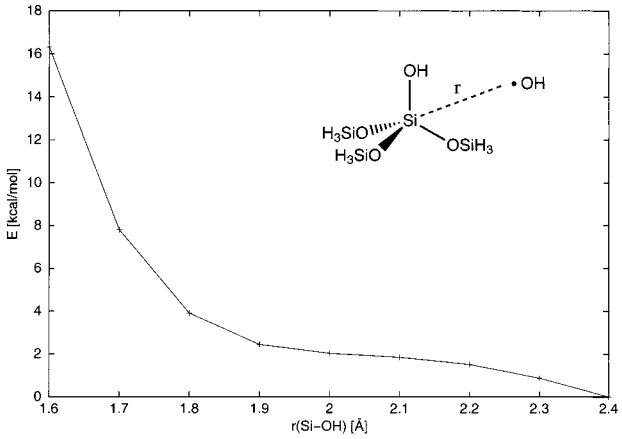

Figure 2. Calculated energy profile for the •OH interaction with the silicon atom site in the isolated silanol cluster as predicted at the B3LYP/6-31G** level of theory. The energy E is given with respect to the total energy of the system at r = 2.4 Å.

SCHEME 3

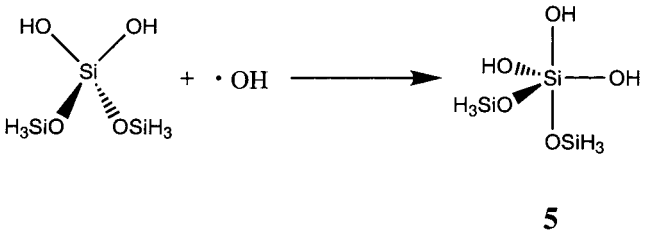

5

barrier is a steric interaction between the incoming hydroxyl radical and the bulky $OSiH_3$ groups. However, the reaction between the hydroxyl radical and geminal silanol cluster silicon atom is energetically favorable, leading to a pentacoordinate silicon complex **5** (Scheme 3). The optimized geometry of the product is shown in Figure 3, and the important structural parameters are shown in Table 2. The reaction energy is −3.5 kcal/mol, and there is no energy barrier to this process as predicted at the B3LYP/6-31G** level of theory. The resulting 5-fold coordinated silicon complex **5** has distorted trigonal bipyramidal geometry with the OH and $SiOH_3$ groups in the axial positions.

While the two equatorial hydroxyls in **5** are fairly strongly bonded to the silicon with normal Si−O bond distances of 1.65 and 1.67 Å, the oxygen−silicon bond in the third, axially coordinated hydroxyl is much weaker, resulting in the Si−O bond length 1.94 Å. Also, both Si−$OSiH_3$ bonds are elongated upon •OH addition. This elongation is more significant in the equatorial Si−$OSiH_3$ bond which is located next to the weakly bonded hydroxyl, from 1.64 Å in the tetrahedral complex **4** to 1.72 Å in **5**. We have also looked for a geometry with both $OSiH_3$ groups in the axial positions, but this configuration is not stable in our calculation. It is interesting to note that the first pentacoordinated silicon compounds with SiO_5 skeletons were experimentally prepared only recently.[32] The ligand configuration around the silicon atom in these synthesized

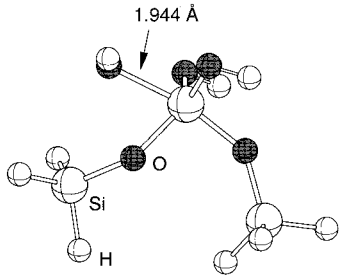

5

Figure 3. Calculated geometry of the 5-coordinated silicon complex **5**.

TABLE 2: Optimized Geometrical Parameters for the 5-Coordinated Silicon Cluster 5 and Transition State Structures 6 and 7 (Bond Lengths in Å and Bond Angles in deg)

	5	6	7
Si−OH	1.666, 1.654, 1.944	1.646, 1.668, 1.737	1.657, 1.722, 1.674
Si−$OSiH_3$	1.694, 1.723	1.667, 2.134	1.647, 2.098
HO−Si−OH	85.6, 86.9, 121.3	92.6, 99.3, 116.2	97.9, 98.9, 121.5
HO_r−Si−$OSiH_3$[a]	70.6, 167.9	65.4, 141.6	104.3, 164.2
H_3SiO−Si−$OSiH_3$	97.3	83.6	87.1
Si−O−SiH_3	138.0, 141.0	128.2, 139.5	126.7, 129.6

[a] HO_r represents the hydroxyl group originating from the reacting hydroxyl radical.

SCHEME 4

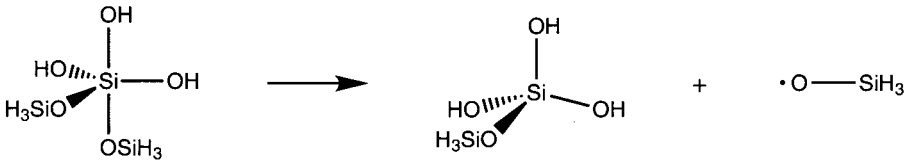

complexes is also a distorted trigonal bipyramid with the axial Si−O bond distances significantly longer (1.798−1.836 Å) than the equatorial ones (1.615−1.665 Å).

The change in the Si−$OSiH_3$ bond lengths upon •OH addition in **5** deserves more consideration. The weaker Si−OH_3 bonds in the pentacoordinated complex **5** will be more susceptible to dissociation than the same bonds in the tetrahedral complex **4**. Because the Si−$OSiH_3$ bond is a model for the Si−O subsurface bond in the real quartz surface, its elongation would correspond to a weakening of the Si−O subsurface bonding upon hydroxyl radical attachment to the surface silicon atom and could lead to disintegration of the surface layer. In fact, a similar pentacoordinated silicon complex has been proposed as an intermediate during OH^- facilitated Si−O subsurface bond dissociation and subsequent silica surface dissolution.[33] Xiao and Lasaga theoretically studied[33] the mechanism of OH^- catalyzed hydrolysis of quartz using cluster models and have predicted the formation of the activated pentacoordinated Si complex to be a rate determining step with energy barrier of 18.9 kcal/mol, which is then followed by the rupture of the Si−OSi bond with a barrier of 4.5 kcal/mol. Similarly, the •OH activated pentacoordinated Si complex **5** could be a precursor for the quartz surface dissolution.

To estimate the energetics involved in the •OH activated Si−$OSiH_3$ bond rupture (Scheme 4), we have attempted to localize a transition state for the •$OSiH_3$ dissociation from the model complex. We have searched for transition state structures for two possible dissociation pathways involving the dissociating $OSiH_3$ group in either *cis* or *trans* positions with respect to the weakly bonded axial OH group. The optimized transition state geometries for dissociation of the *cis*-$OSiH_3$ (**7**) and *trans*-$OSiH_3$ (**7**) groups are presented in Figure 4, and important geometrical parameters are in Table 2.

The overall reaction energy is −4.0 kcal/mol, and the energy barrier to the process is 8.4 and 4.4 kcal/mol for the *cis*- and *trans*-$OSiH_3$ dissociation, respectively. These barriers are substantially lower than the calculated energy barrier in the rate determining step in the OH^- catalyzed Si−$OSiH_3$ bond dissociation (18.9 kcal/mol).[33] The calculated potential energy surface (PES) for the *trans*-$OSiH_3$ dissociation is presented in Figure 5. The PES was determined by varying two geometrical parameters, *r*(Si−OH) and *r*(Si−*trans*-$OSiH_3$) in **5**. The calculated energy surface is fairly flat, and the transition state geometry **7** is only 4.4 kcal/mol above the starting structure **5**. Inspection of the calculated PES shows that for the 5-coordinated complex **5** to reach the transition state the Si−OH bond is shortened first followed by the Si−$OSiH_3$ bond elongation. This implies a stepwise rather than a synchronous mechanism of the Si−$OSiH_3$ bond dissociation.

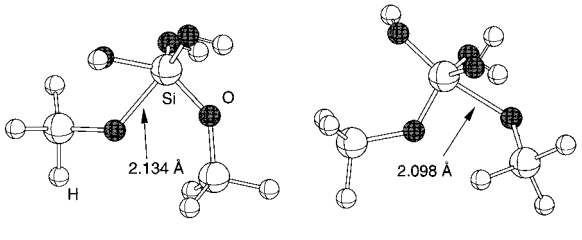

6 **7**

Figure 4. Optimized transition state geometries for the *cis*- (**6**) and *trans*-$OSiH_3$ (**7**) group dissociation from **5**, respectively.

The Si−$OSiH_3$ bond in the lower energy transition state geometry **7** is elongated from 1.72 to 2.10 Å. While the Si−$OSiH_3$ bond is being stretched, the longer Si−OH bond (Si−OH distance of 1.94 Å in **5**) is being strengthened and shortened, resulting in the Si−OH bond length of 1.67 Å.

The overall calculated reaction coordinate for the hydroxyl radical activated *trans*-Si−$OSiH_3$ bond dissociation is shown in Figure 6. Because the surrounding crystal lattice-imposed strain on the active surface site on the real surface may alter somewhat the energy barrier to the Si−O bond dissociation, it will be of interest to investigate this effect by using extended three-dimensional periodic slab models of the surface which include long-range lattice effects.

These cluster model results suggest that hydroxyl radical adsorption on the surface can significantly lower the barrier to surface dissolution compared to that for the OH^- catalyzed process. The product of the hydroxyl radical-activated subsurface Si−O dissociation is a reactive siloxyl radical, Si−O•. The generation of these radical species may have a profound effect on toxicity of the quartz surface, because the surface silicon radicals will be in the near vicinity of adsorbed cellular material where they can not only effectively inflict oxidative damage but also participate in regeneration of •OH radicals. However, other factors such as the hydrophilic and hydrophobic properties of the surface which determine the extent of protein adsorption will also play a role in the membranolytic activity of the quartz surface. These processes may also be modulated by coadsorbed phospholipids, the major component of pulmonary surfactant, as observed experimentally.[34−38]

It is also interesting to note the difference between the reactivities of the surface silicon atom sites in the isolated and geminal silanols toward •OH. The computational results imply

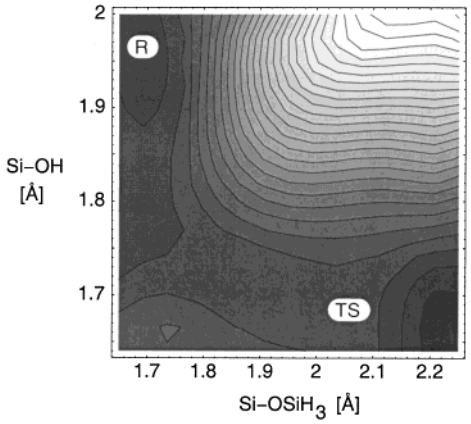

Figure 5. Contour plot of the calculated potential energy surface for the *trans*-$OSiH_3$ group dissociation from **5**. The approximate locations of the reactant **5** (R) and transition state **7** (TS) are shown. The darker gray levels correspond to areas with lower energy. Contours are separated by 2 kcal/mol.

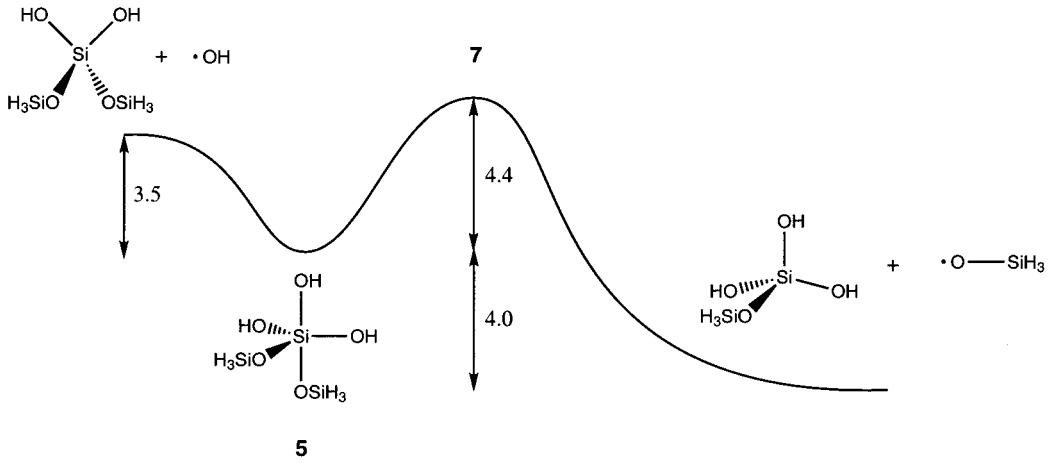

Figure 6. Schematic reaction coordinate for the •OH activated *trans*-Si−$OSiH_3$ bond dissociation. The energy values are in kcal/mol as predicted at the B3LYP/6−31G** level.

that the quartz surface dissolution would preferably take place at the geminal silanol site. Although the isolated silanol cluster model predicts no favorable interaction between the Si site and •OH, the exact energetics of the process can be affected by the specific site geometry and also by hydrogen bonding between adjacent silanols on the real surface.[39] This is supported by our preliminary modeling of the same reaction, using an extended three-dimensional periodic slab model where the calculations predict a favorable interaction between •OH and not only the geminal silanol sites but also some isolated silanol surface sites.[40]

We have also considered the possibility of another competing reaction involving •OH, a hydroxyl radical interaction with the oxygen in a siloxane bridge (Si−O−Si). Our calculations show, not surprisingly, that there is a repulsive interaction between the siloxane oxygen and the oxygen atom of the hydroxyl radical. The preferable way of interacting is the formation of a weakly bonded complex where the hydroxyl radical is coordinated to the siloxane bridge oxygen by its hydrogen atom. The reaction energies for formation of these complexes are −6.8 and −2.0 kcal/mol for the isolated and geminal silanol clusters, respectively. The reaction energy for the isolated silanol cluster is higher because of auxiliary hydrogen bonding of the attacking •OH to the neighboring silanol.

Conclusions

We have theoretically studied the interaction between a hydroxyl radical and a silanol-terminated quartz surface using two molecular cluster models. The two clusters represent experimentally observed surface silanol configurations: the isolated and geminal silanols. The hydroxyl radical weakly binds to a hydrogen atom of the silanol group in both models. The possible silanol hydrogen atom abstraction by •OH and the formation of Si−O• radical are energetically unfavorable by 8 kcal/mol in our calculation. The •OH interacts differently with the central Si atom in the isolated and geminal silanol cluster models which approximate the silicon site on the surface. While •OH does not bind to the silicon atom in the isolated silanol cluster, probably because of steric effects, it reacts with Si in the geminal silanol complex. The product of this reaction is a 5-coordinated silicon complex. The Si−$OSiH_3$ bonds in this complex, which represent the Si−O subsurface bonds in the real quartz surface, are weakened and are susceptible to dissociation. The dissociation is an exothermic process (−4 kcal/mol) with an energy barrier of only 4 kcal/mol. One of the products of this dissociation is a free radical complex H_3Si−O•. The energy barrier in the rate determining step for the Si−$OSiH_3$ bond dissociation is substantially lower than the barrier in the OH^- catalyzed process.

This proposed subsurface Si−O bond dissociation mechanism suggests a possible pathway for reactivation of a fairly chemically inert silanol terminated quartz surface. The adsorption of •OH on the surface and subsequent Si−O dissociation can lead to the generation of surface silicon-based radicals which may then participate in further radical propagation reactions. Because free radical species are thought to play a major role in silica toxicity, this surface reactivation followed by the formation of surface-based radicals could have implications for elucidation of the detailed toxicity mechanism of aged, silanol-terminated silica.

Long-range effects, crystal lattice constraints, and neighboring silanol interactions may somewhat influence the predicted reaction energetics. The extent of these effects is the subject of our next study using three-dimensional periodic slab models of the surface.

Acknowledgment. The author wishes to thank William E. Wallace, Sid Soderholm, and Vincent Castranova for stimulating and fruitful discussions and NIOSH for the research opportunity.

References and Notes

(1) *IARC Monographs on the Evaluation of the Carcinogenic Risk of Chemicals to Humans: Silica, Some Silicates, Coal Dust and para-Aramid Fibrils*; International Agency for Research on Cancer: Lyon, France, 1997; Vol. 68.

(2) Fubini, B.; Bolis, V.; Giamello, E. *Inorg. Chim. Acta* **1987**, *138*, 193−197.

(3) Vallyathan, V.; Shi, X.; Dalal, N. S.; Irr, W.; Castranova, V. *Am. Rev. Respir. Dis.* **1988**, *138*, 1213−1219.

(4) Fubini, B.; Giamello, E.; Volante, M. *Inorg. Chim. Acta* **1989**, *162*, 187−189.

(5) Fubini, B.; Giamello, E.; Pugliese, L.; Volante, M. *Solid State Ionics* **1989**, *32/33*, 334−343.

(6) Driscoll, K. E.; Higgins, J. M.; Leytart, M. J.; Crosby, L. L. *Toxicol. in Vitro* **1990**, *4*, 284−288.

(7) Fubini, B.; Giamello, E.; Volante, M.; Bolis, V. *Toxicol. Ind. Health* **1990**, *6*, 571−598.

(8) Vallyathan, V.; Kang, J. H.; Van Dyke, K.; Dalal, N. S.; Castranova, V. *J. Toxicol. Environ. Health* **1991**, *33*, 303−315.

(9) Costa, D.; Fubini, B.; Giamello, E.; Volante, M. *Can. J. Chem.* **1991**, *69*, 1427−1434.

(10) Janssen, Y. M. W.; Marsh, J. P.; Absher, M. P.; Hemenway, D.; Vacek, P. M.; Lelie, K. O.; Borm, P. J. A.; Mossman, B. T. *J. Biol. Chem.* **1992**, *267*, 10625−10630.

(11) Fubini, B.; Bolis, V.; Cavenago, A.; Volante, M. *Scand. J. Work, Environ. Health* **1995**, *21 suppl 2*, 9−14.

(12) Castranova, V.; Dalal, N. S.; Vallyathan, V. In *Silica and Silica-induced Lung Diseases*; Castranova, V., Vallyathan, V., Wallace, W. E., Eds.; CRC Press: Boca Raton, FL, 1996; pp 91−105.

(13) Castranova, V.; Pailes, W. H.; Dalal, N. S.; Miles, P. R.; Bowman, L.; Vallyathan, V.; Pack, D.; Weber, K. C.; Hubbs, A.; Schwegler-Berry, D.; Xiang, J.; Dey, R.; Blackford, J.; Ma, J. Y. C.; Barger, M.; Shoemaker, D. A.; Pretty, J. R.; Ramsey, D. M.; McLaurin, J. L.; Khan, A.; Baron, P. A.; Childress, C. P.; Stettler, L. E.; Teass, A. W. *Appl. Occup. Environ. Hyg.* **1996**, *11*, 937−941.

(14) Castranova, V.; Antonini, J. M.; Reasor, M. J.; Wu, L.; VanDyke, K. In *Silica and Silica-induced Lung Diseases*; Castranova, V., Vallyathan, V., Wallace, W. E., Eds.; CRC Press: Boca Raton, FL, 1996; pp 185−195.

(15) Fubini, B.; Otero Areán, C. *Chem. Soc. Rev.* **1999**, *28*, 373−381.

(16) Elias, Z.; Poirot, O.; Daniére, M. C.; Terzetti, F.; Marande, A. M.; Dzwigaj, S.; Pezerat, H.; Fenoglio, I.; Fubini, B. *Toxicol. in Vitro* **2000**, *14*, 409−422.

(17) Guthrie, G. D., Jr.; Heaney, P. J. *Scand. J. Work, Environ. Health* **1995**, *21 suppl. 2*, 5−8.

(18) Shoemaker, D. A.; Pretty, J. R.; Ramsey, D. M.; McLaurin, J. L.; Khan, A.; Teass, A. W.; Castranova, V.; Pailes, W. H.; Dalal, N. S.; Miles, P. R.; Bowman, L.; Leonard, S.; Shumaker, J.; Vallyathan, V.; Pack, D. *Scand. J. Work, Environ. Health* **1995**, *21 suppl 2*, 15−18.

(19) Sauer, J.; Ugliengo, P.; Garrone, E.; Saunders, V. R. *Chem. Rev.* **1994**, *94*, 2095−2160.

(20) Gibbs, G. V.; Downs, J. W.; Boisen, M. B., Jr. In *Reviews in Mineralogy*; Heaney, P. J., Prewitt, C. T., Gibbs, G. V., Eds.; MSA: Washington, DC, 1994; Vol. 29, pp 331−368.

(21) Casanovas, J.; Illas, F.; Pacchioni, G. *Chem. Phys. Lett.* **2000**, *326*, 523−529.

(22) Sneh, O.; George, S. M. *J. Phys. Chem.* **1995**, *99*, 4639−4647.

(23) Chuang, I.; Maciel, G. E. *J. Am. Chem. Soc.* **1996**, *118*, 401−406.

(24) Chuang, I.; Maciel, G. E. *J. Phys. Chem. B* **1997**, *101*, 3052−3064.

(25) Ferrari, A. M.; Ugliengo, P.; Garrone, E. *J. Phys. Chem.* **1993**, *97*, 2671−2676.

(26) Lee, C.; Yang, W.; Parr, R. G. *Phys. Rev. B* **1988**, *37*, 785−789.

(27) Becke, A. D. *J. Chem. Phys.* **1993**, *98*, 1372−1377.

(28) Schlegel, H. B. *J. Comput. Chem.* **1982**, *3*, 214−218.

(29) Frisch, M. J.; Trucks, G. W.; Schlegel, H. B.; Scuseria, G. E.; Stratmann, R. E.; Burant, J. C.; Dapprich, S.; Millam, J. M.; Daniels, A. D.; Kudin, K. N.; Strain, M. C.; Farkas, O.; Tomasi, J.; Barone, V.; Cossi, M.; Cammi, R.; Mennucci, B.; Pomelli, C.; Adamo, C.; Clifford, S.; Ochterski, J.; Cui, Q.; Morokuma, K.; Malick, D. K.; Rabuck, A. D.; Liu, G.; Liashenko, A.; Piskorz, P.; Komaromi, I.; Gill, P. M. W.; Johnson, B. G.; Robb, M. A.; Cheeseman, J. R.; Keith, T. A.; Petersson, G. A.; Montgomery, J. A.; Raghavachari, K.; Al-Laham, M. A.; Zakrzewski, V. G.; Ortiz, J. V.; Foresman, J. B.; Cioslowski, J.; Stefanov, B. B.; Nanayakkara, A.; Challacombe, M.; Peng, C. Y.; Ayala, P. Y.; Chen, W.; Wong, M. W.; Andres, J. L.; Replogle, E. S.; Gomperts, R.; Martin, R. L.; Fox, D. J.; Head-Gordon, M.; Gonzales, C.; Pople, J. A. *Gaussian 98*, Revision A.7; Gaussian, Inc.: Pittsburgh, PA, 1998.

(30) March, J. In *Advanced Organic Chemistry*, 3rd ed.; John Wiley & Sons: New York, 1985; Chapter 14, p 609.

(31) Levien, L.; Prewitt, C. T. *Am. Mineral.* **1981**, *66*, 324−333.

(32) Tacke, R.; Burschka, C.; Richter, I.; Wagner, B.; Willeke, R. *J. Am. Chem. Soc.* **2000**, *122*, 8480−8485.

(33) Xiao, Y.; Lasaga, A. C. *Geochim. Cosmochim. Acta* **1996**, *60*, 2283−2295.

(34) Wallace, W. E.; Keane, M. J.; Mike, P. S.; Hill, C. A.; Vallyathan, V.; Regad, E. D. *J. Toxicol. Environ. Health* **1992**, *37*, 391−409.

(35) Hill, C. A.; Wallace, W. E.; Keane, M. J.; Mike, P. *Cell Biol. Toxicol.* **1995**, *11*, 119−128.

(36) Wallace, W. E.; Keane, M. J.; Harrison, J. C.; Stephens, J. W.; Brower, P. S.; Grayson, R. L.; Attfield, M. D. In *Silica and Silica-induced Lung Diseases*; Castranova, V., Vallyathan, V., Wallace, W. E., Eds.; CRC Press: Boca Raton, FL, 1996; pp 107−117.

(37) Keane, M. J.; Wallace, W. E. In *Silica and Silica-induced Lung Diseases*; Castranova, V., Vallyathan, V., Wallace, W. E., Eds.; CRC Press: Boca Raton, FL, 1996; pp 271−281.

(38) Fubini, B.; Wallace, W. E. In *Adsorption on Silica Surfaces*; Papirer, E., Ed.; Marcel Dekker: New York, 2000; pp 645−664.

(39) Pelmenschikov, A.; Strandh, H.; Pettersson, L. G. M.; Leszczynski, J. *J. Phys. Chem. B* **2000**, *104*, 5779−5783.

(40) Konecny, R. Manuscript in preparation.